UCLA
UCLA Previously Published Works

Title
Assessing Consistency in Fuel Consumed Between Activity-Based Wildfire Emission Estimates

Permalink
https://escholarship.org/uc/item/7th4d133

Journal
Geophysical Research Letters, 53(8)

ISSN
0094-8276

Authors
Saide, PE
Wu, Y
Arnold, M
et al.

Publication Date
2026-04-28

DOI
10.1029/2025gl120030

Copyright Information
This work is made available under the terms of a Creative Commons Attribution License, available at https://creativecommons.org/licenses/by/4.0/

Peer reviewed

eScholarship.org Powered by the California Digital Library
University of California

Check for updates

AGU ADVANCING EARTH AND SPACE SCIENCES

Geophysical Research Letters

RESEARCH LETTER
10.1029/2025GL120030

Special Collection:
Biomass Burning Uncertainties: Emissions, Chemistry, and Physics

Key Points:

- Large differences (factors 2–16 on the mean) in fuel consumed for emissions estimates across burn severity classes are explained
- Fuel consumed increases with burn severity across all approaches except for the energy-based approach for forest cover
- Fire radiative power corrections that account for canopy and smoke shading during extreme fire behavior likely need to be developed

Supporting Information:

Supporting Information may be found in the online version of this article.

Correspondence to:
P. E. Saide,
saide@atmos.ucla.edu

Citation:
Saide, P. E., Wu, Y., Arnold, M., Thapa, L. H., Soja, A., Gargulinski, E., et al. (2026). Assessing consistency in fuel consumed between activity-based wildfire emission estimates. *Geophysical Research Letters*, *53*, e2025GL120030. https://doi.org/10.1029/2025GL120030

Received 16 OCT 2025
Accepted 1 APR 2026

Author Contributions:
Conceptualization: P. E. Saide
Data curation: P. E. Saide, M. Arnold, L. H. Thapa, A. Soja, E. Gargulinski, F. Li, C. Wiedinmyer, L. K. Emmons, W. Tang, A. L. Westerling, Q. Xu, E. M. Ordway, N. Queally, L. Kueppers
Formal analysis: P. E. Saide, Y. Wu
Funding acquisition: P. E. Saide, E. M. Ordway, L. Kueppers
Investigation: P. E. Saide

© 2026 The Author(s).
This is an open access article under the terms of the Creative Commons Attribution-NonCommercial License, which permits use, distribution and reproduction in any medium, provided the original work is properly cited and is not used for commercial purposes.

Assessing Consistency in Fuel Consumed Between Activity-Based Wildfire Emission Estimates

P. E. Saide[1,2], Y. Wu[1], M. Arnold[1], L. H. Thapa[1,3], A. Soja[4,5], E. Gargulinski[5], F. Li[6], C. Wiedinmyer[7], L. K. Emmons[8], W. Tang[8], A. L. Westerling[9], Q. Xu[9], E. M. Ordway[2,10], N. Queally[10], and L. Kueppers[11]

[1]Department of Atmospheric and Oceanic Sciences, University of California—Los Angeles, Los Angeles, CA, USA, [2]Institute of the Environment and Sustainability, University of California—Los Angeles, Los Angeles, CA, USA, [3]Now at Colorado State University, Fort Collins, CO, USA, [4]NASA Langley Research Center, Hampton, VA, USA, [5]National Institute of Aerospace, Hampton, VA, USA, [6]Department of Geography and Geospatial Sciences, South Dakota State University, Brookings, SD, USA, [7]University Corporation for Atmospheric Research, Boulder, CO, USA, [8]Atmospheric Chemistry Observations and Modeling Laboratory, NSF National Center for Atmospheric Research (NCAR), Boulder, CO, USA, [9]Sierra Nevada Research Institute, University of California Merced, Merced, CA, USA, [10]Department of Ecology and Evolutionary Biology, University of California—Los Angeles, Los Angeles, CA, USA, [11]Energy and Resources Group, University of California, Berkeley, and Lawrence Berkeley National Laboratory, Berkeley, CA, USA

Abstract Wildfire emission inventories exhibit large variability that complicates assessments of smoke impacts. Here we compare fuel consumed (in mass per burned area units) from multiple burn area-based and energy-based approaches for fires in the western US during 2020. Average fuel consumed can vary by up to factors of 2–16 between approaches across burn severity classes and fuel types. Fuel consumed estimates typically increase with burn severity, except for the energy-based approaches for forest land cover, where it decreases for high burn severity. Also, in contrast to other approaches, energy-based estimates decrease for tree cover greater than 40% regardless of burn severity class. This implies that corrections to the energy-based approach are likely needed across burn severity categories to account for canopy and smoke shading. The methodological recommendations provided would likely result in greater consistency between wildfire emission estimates and highlight the need to better constrain fuel loading and consumption.

Plain Language Summary Estimates of smoke emitted into the atmosphere can be highly variable, which can result in uncertainties when estimating smoke impacts. Fuel consumption is one of the primary drivers for this variability. Here, we compare different methods to estimate fuel consumption for fires in the western US in 2020. We find that the different methods result in large variability in fuel consumed estimates, with a factor of 10 or larger differences commonly found. For grasslands, shrublands and savannas, all estimation methods show an increase in fuel consumed as the fire burn severity increases, which is consistent with the expectation that the more severe the fire, the more fuel is consumed. However, approaches based on observing the energy radiated from the fire and relating that to fuel consumed shows the opposite tendency over forests, especially for areas with dense tree cover, which is against expectations. This likely indicates that corrections to account for the energy that cannot penetrate the canopy or that gets absorbed by the combustion gases need to be implemented. We provide recommendations to improve estimates of fuel consumption that we expect will reduce the uncertainty in smoke emission estimates.

1. Introduction

Multiple approaches have been developed to estimate fire emissions. Activity-based approaches estimate the mass of fuel consumed by fires and convert it into chemical constituents using emission factors (Andreae, 2019; Seiler & Crutzen, 1980). Two activity-based approaches are regularly used to estimate the fuel consumed. The burn area-based approach, also referred to as inventory-based, bottom-up, or the indirect combustion approach (French & Hudak, 2023; Parrington et al., 2025), requires estimates of burn area, fuel loading, and fraction of fuel burned to estimate fuel consumed. Examples of this approach include the Fire INventory from National Center for Atmospheric Research (FINN, Wiedinmyer et al., 2023), the Global Fire Emissions Database (GFED, van der Werf et al., 2017), the Bluesky framework (Larkin et al., 2009), the Wildfire Burn Severity and Emissions inventory (WBSE, Xu et al., 2022), and the Fuel Characteristic Classification System (FCCS)/Fuel2Fire (formerly WEB-FE) emissions used in the Real-time Air Quality Modeling System (RAQMS) (Petrenko et al., 2012; Pierce

19448007, 2026, 8, Downloaded from https://agupubs.onlinelibrary.wiley.com/doi/10.1029/2025GL120030 by Elsa M. Ordway - University Of California, Los Angeles , Wiley Online Library on [10/05/2026]. See the Terms and Conditions (https://onlinelibrary.wiley.com/terms-and-conditions) on Wiley Online Library for rules of use; OA articles are governed by the applicable Creative Commons License

Methodology: P. E. Saide
Project administration: P. E. Saide, E. M. Ordway, L. Kueppers
Resources: P. E. Saide, M. Arnold, L. H. Thapa
Software: P. E. Saide, M. Arnold, L. H. Thapa
Supervision: E. M. Ordway, L. Kueppers
Validation: P. E. Saide
Visualization: P. E. Saide
Writing – original draft: P. E. Saide
Writing – review & editing: P. E. Saide, L. H. Thapa, A. Soja, E. Gargulinski, F. Li, C. Wiedinmyer, L. K. Emmons, W. Tang, A. L. Westerling, Q. Xu, E. M. Ordway, N. Queally, L. Kueppers

et al., 2007; Soja et al., 2004). The energy-based approach, also referred to as the fire radiative power (FRP)-based, top-down, combustion, or direct approach (French & Hudak, 2023; Parrington et al., 2025), estimates fuel consumed directly from observed fire radiative energy (FRE, the amount of energy radiated during the combustion process and the time integral of FRP) by converting it to a mass of dry fuel consumed using a combustion factor (mass/energy, Wooster et al., 2005). Examples of systems using this approach include The Quick Fire Emissions Data set (QFED, Darmenov & da Silva, 2015), the Global Fire Assimilation System (GFAS, Kaiser et al., 2012), and the Fire Energetics and Emissions Research (FEER, Ichoku & Ellison, 2014). While initial versions of these energy-based systems use FRP from low-earth orbiting satellites, forthcoming updates and recent algorithms such as the Regional ABI and VIIRS fire Emissions (RAVE, Li et al., 2022) leverage geostationary satellites to provide hourly estimates of FRP, FRE, and emissions.

There is a large body of literature comparing fire emissions inventories at multiple scales, from global (e.g., Pan et al., 2020; Shi et al., 2015; Wiedinmyer et al., 2023), to regional (Bekker et al., 2025; Byrne et al., 2024; Carter et al., 2020; Xu et al., 2022; Zhang et al., 2014), and down to the scale of single fires (Stockwell et al., 2022; Wiggins et al., 2021; Ye et al., 2021), with the general finding that emission estimates vary highly across modeling systems with factor of 2–3 differences being common (Parrington et al., 2025), which can result in large variability when assessing the impacts of smoke. Sources of uncertainty are many including the use of different emission factors, source of fire detections (which can influence missing small fires or cloud-covered fires), burn area or severity estimates (in the case of burn area-based), combustion factors (in the case of energy-based), and tunning factors to improve agreement with atmospheric observations (e.g., Darmenov & da Silva, 2015; Kaiser et al., 2012), which complicate the understanding of the differences across the emission estimation methods. Estimating fuel consumption is a key step to calculate fire emissions and, while some studies have compared it between approaches (e.g., Larkin et al., 2009), comparisons across multiple methodologies typically used to predict smoke and uncertainty quantification are lacking.

In this study we compare the fuel consumed (in units of mass of fuel consumed per unit burned area) estimated by one energy-based approach and four burn area-based approaches. This is done for fires on the 2nd half of 2020, which include the record-breaking western US wildfires that burned over 40,000 km^2 and had substantial air quality impacts (Li, Tong, et al., 2021). We estimate fuel consumed on a fixed grid aggregated over the lifetime of the fires and compare statistics between approaches as a function of fire and landscape characteristics. This allows us to better quantify the differences in modeled fuel consumption estimates and identify opportunities for improvement. Section 2 presents the data sets used and describes the fire emission methodologies used, Section 3 shows results and discussions derived from comparing the fuel consumed estimates, and Section 4 provides conclusions and future directions.

2. Data and Methods

General information about data sets used, including acronym definitions and references, is summarized in Table S1 of Supporting Information S1. For this investigation, we compiled and estimated fuel consumed for all wildfires greater than 10 km^2 in the western and central continental U.S. between 1st July and 1st December of 2020, resulting in 164 fires (see map in Figure S1 in Supporting Information S1) that allow for robust statistics. Examples of the different input and derived data sets for the Creek fire, an historical fire that has been thoroughly studied (Lee et al., 2023; Mattarochia, 2022; Safford et al., 2022), is shown in Figures S2 and S3 of Supporting Information S1. In the following subsections a brief description of the methodologies used to compute fuel consumed is presented.

2.1. RAVE Fuel Consumed

RAVE provides hourly FRP across the continental U.S. from geostationary and low-earth orbiting satellites (Table S1 in Supporting Information S1) with the algorithm described in detail by Li et al. (2022). The FRP, gridded at the RAVE native 3 km resolution, is integrated over the study period to obtain gridded cumulative FRE (Figure S2d in Supporting Information S1). Following the RAVE algorithm, total fuel burned (mass units) per grid is obtained by applying a combustion factor of 0.368 kg fuel/MJ. Burn severity from the Monitoring Trends in Burn Severity (MTBS) data set (Table S1, Figure S2a in Supporting Information S1) is derived from pre- and post-fire imagery and characterizes the location, extent, and severity of all large fires within the US (Eidenshink et al., 2007). This is used to estimate burn area within each RAVE grid cell (Figure S2b in Supporting

10.1029/2025GL120030

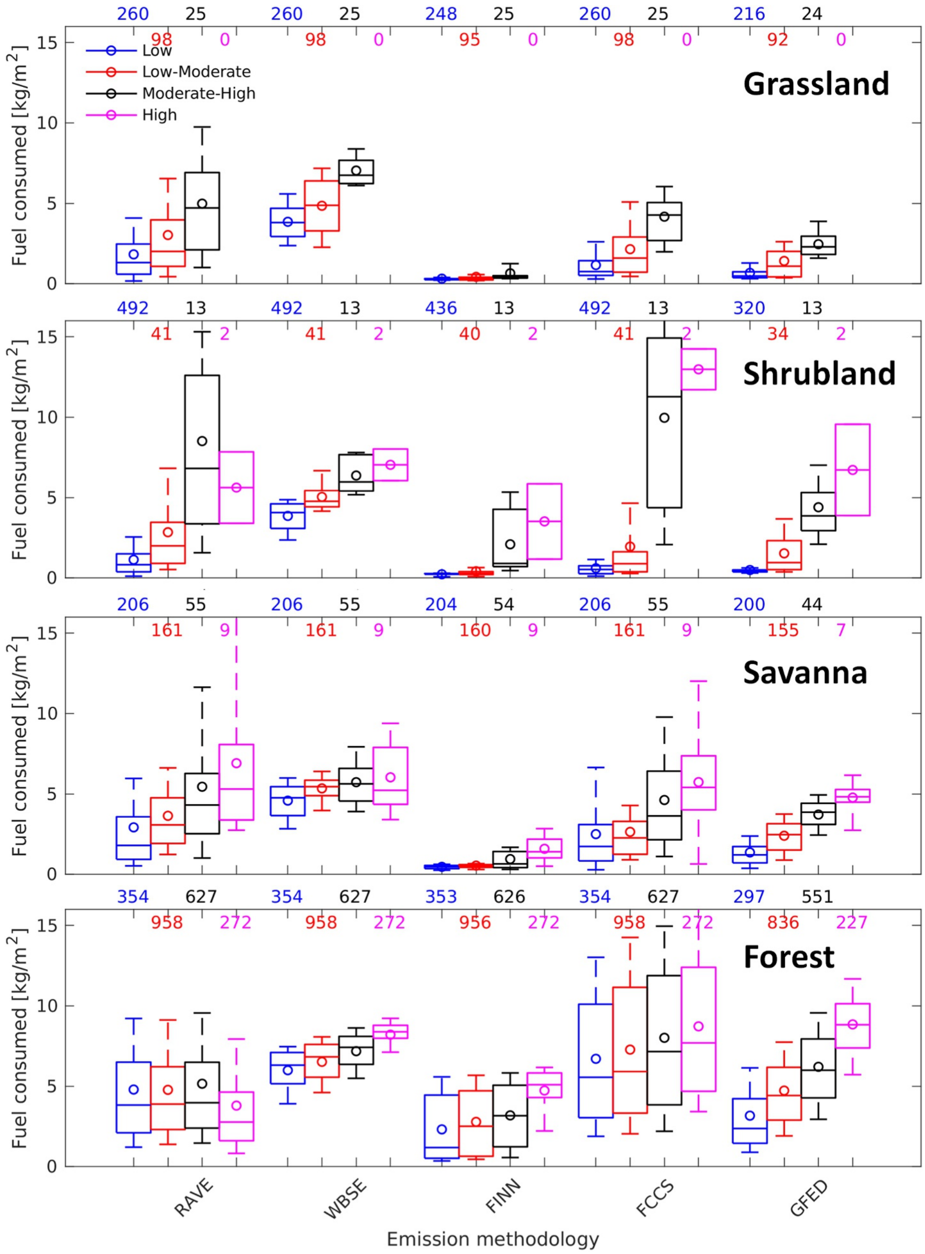

Figure 1. Box and whisker plots showing fuel consumed (y-axis) as a function of burn severity class (colors) for each methodology (x-axis) for RAVE grid cells with different dominant land cover as classified in RAVE. Center solid lines indicate the median, circles represent the mean, boxes indicate upper and lower quartiles, and whiskers show the upper and lower deciles. Number of RAVE grid cells used to calculate statistics is shown on top of each panel using the corresponding color.

Information S1) by adding the area covered by "low," "moderate" and "high" severity pixels (assuming 30×30 m^2 area per pixel), excluding pixels in the "unburned to low" category as in previous work (Williams et al., 2025). RAVE fuel consumed in kg/m^2 is then obtained by the ratio of total fuel burned per grid and burn area (Figure S2e in Supporting Information S1). Grid cells with a burn area below 25% of the total are excluded from the analysis to avoid generation of outliers.

The 3×3 km^2 RAVE grid is used as a basis for comparing methods to estimate fuel consumed, resulting in 3,573 grid cells with valid data when aggregating all fires (Figures 1 and 2). Each RAVE grid cell has a dominant land cover assigned based on the 2019 MODIS LCT IGBP classification (Table S1, Figure S1 in Supporting

19448007, 2026, 8, Downloaded from https://agupubs.onlinelibrary.wiley.com/doi/10.1029/2025GL120030 by Elsa M. Ordway - University Of California, Los Angeles , Wiley Online Library on [10/05/2026]. See the Terms and Conditions (https://onlinelibrary.wiley.com/terms-and-conditions) on Wiley Online Library for rules of use; OA articles are governed by the applicable Creative Commons License

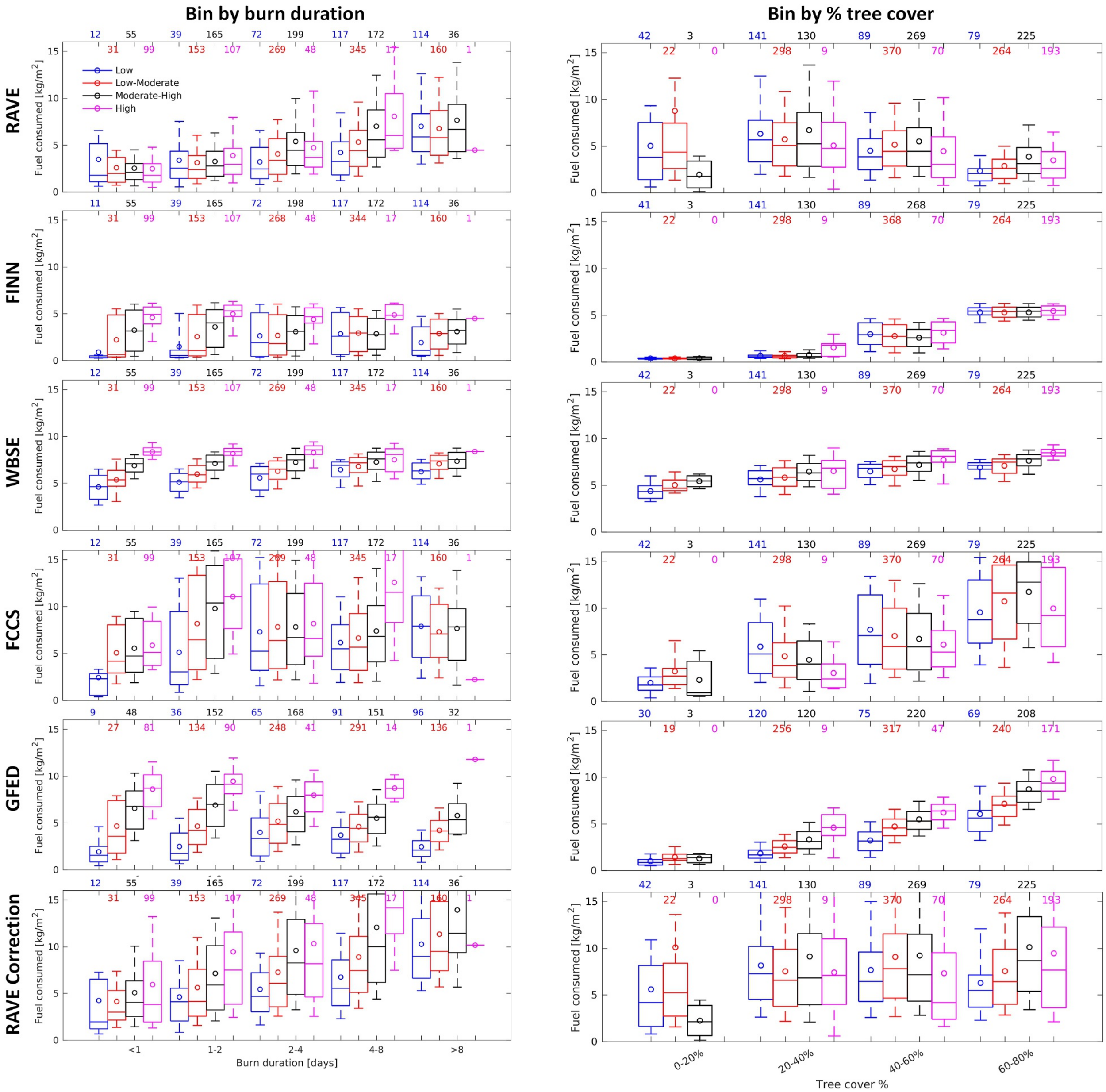

Figure 2. Like Figure 1 but only for forest land cover, binning by RAVE fire duration (left column) and by NLCD tree cover (right column), with colors representing ranges of burn severity classes. Different approaches to estimate fuel consumed are shown in rows.

Information S1) as described on Li et al. (2022). The average burn severity per RAVE grid cell is calculated assigning values of 2, 3, and 4 to MTBS pixels with "low," "moderate" and "high" burn severity, respectively, and taking the average within the RAVE grid cell (Figure S2c in Supporting Information S1). Categories at the RAVE grid of "low," "low-moderate," "moderate-high" and "high" are assigned to averages between 2 and 2.5, 2.5–3, 3–3.5, and 3.5–4, respectively. Similarly, each RAVE grid cell is assigned a % tree cover by averaging the underlying 30 m NLCD TCC data set (Table S1, Figure S2g in Supporting Information S1) to the RAVE grid (Figure S2h in Supporting Information S1). Additionally, we estimate the burn duration by counting the hours of FRP values above zero in each RAVE grid cell during the study period (Figure S2f in Supporting Information S1). We use these variables to assess behavior by fuel type, burn severity, tree cover and burn duration (see Section 3), and to compare trends between them (e.g., Figure S4 in Supporting Information S1). RAVE is the only energy-based approach compared to burn area-based methodologies as other approaches are typically provided in grids of

19448007, 2026, 8, Downloaded from https://agupubs.onlinelibrary.wiley.com/doi/10.1029/2025GL120030 by Elsa M. Ordway - University Of California, Los Angeles , Wiley Online Library on [10/05/2026]. See the Terms and Conditions (https://onlinelibrary.wiley.com/terms-and-conditions) on Wiley Online Library for rules of use; OA articles are governed by the applicable Creative Commons License

0.1° resolution of coarser (Darmenov & da Silva, 2015; Kaiser et al., 2012), which if used as the reference grid reduces the sample size significantly (Figure S5 in Supporting Information S1).

2.2. FINN Fuel Consumed

The FINNv2.5 methodology is described by Wiedinmyer et al. (2023). FINN output files provide fuel consumed (kg/m^2) and burn area (m^2) daily at 1 km resolution, from where daily total fuel burned (kg) can be estimated. We aggregated the total fuel burned and burn area to the RAVE grid and took the ratio of the two to find the aggregated fuel consumed in kg/m^2 (Figure S2j in Supporting Information S1). The FINN methodology was replicated to derive the fuel consumed based on the fuel loads and fraction consumed described by Wiedinmyer et al. (2011, 2023), obtaining similar results as those from the FINN output files. The FINN methodology assigns fuel loading into two vegetation types: coarse/woody and herbaceous, with the herbaceous loads having values below 1 kg/m^2 for all land covers. When the fire pixel has more than 40% tree cover (based on MODIS VCF, see Table S1 and Figure S2i in Supporting Information S1), FINN assumes that 30% of coarse/woody vegetation is consumed and none otherwise. Fuel consumed is then calculated as the product of the fractional cover of each vegetation type, the fraction of biomass that is burned, and the corresponding fuel loading. Note that while FINN uses a different tree cover data set than what is used to classify RAVE gridcells, they are comparable when aggregated to the RAVE grid (Figures S2g and S2i in Supporting Information S1), with NLCD typically showing larger values for denser tree cover.

2.3. WBSE Fuel Consumed

Another method of fuel consumption estimation is determined following the approach from Wildfire Burn Severity and Emissions inventory (WBSE) proposed by Xu et al. (2022). With the objective to use these emissions in projected climate scenarios (which restricts the variables available to be used as inputs), Landfire's EVT (Table S1 in Supporting Information S1) categories are simplified by cross-walking them to 5 fuel categories (grassland, shrubland, and forests at elevations below 5,500 ft, above 7,500 ft, and in between) and the fuel consumed is assigned as a function of burn severity for forest classes (4.5–7.5 kg/m^2 for low severity up to 6.2–10.1 kg/m^2 for high severity) and constant for grassland (0.4 kg/m^2) and shrubs (4.7 kg/m^2) (Figure S2k in Supporting Information S1). Land covers that do not match any of the above classes are assigned zero fuel consumed. The fuel consumed is then averaged within each RAVE grid cell containing fires (Figure S2l in Supporting Information S1). While Xu et al. (2022) derived burn severity for estimating fuel consumed over California, here we use MTBS burn severity to provide a control on variability arising from differences in burn severity estimates. Note that the use of different land use data sets can lead to mismatches in the fuel classification (e.g., Figure S6 in Supporting Information S1) that can influence fuel consumed as shown in the Results.

2.4. FCCS/Fire2Fuel Fuel Consumed

Another method used to estimate fuel consumed was developed to estimate emissions for the FIREX-AQ field campaign by the Fuel2Fire team (Warneke et al., 2023). FCCS provides fuel load estimates for a variety of fuel beds that are based on a combination of best-available ground-based data, remotely-sensed LiDar, satellite data and models (Ottmar et al., 2007; Riccardi et al., 2007). The six fuel bed strata includes: canopy, shrub, herbaceous, wood (e.g., downed, stumps, and piles), LLM (litter, lichen and moss) and ground fuels (e.g., duff). The LANDFIRE extended team produces "Updated" data at least annually and a complete "Remap" every 3–4 years. For the FIREX-AQ campaign, the Fuel2Fire team used the 2014 Remap to generate five 30 m resolution potential fuel consumed databases providing the amount of fuel that would be available to burn, dependent on the five National Fire Danger Rating System potential for different fire-weather risks (low to extreme, Figures S3a–S3e in Supporting Information S1). For this we use the daily Severe Fire Danger Index (SFDI, Jolly et al., 2019), calculated using a 40-year fire index climatology (1979–2018) provided by the CEMS (Table S1 in Supporting Information S1). SFDI was assigned per RAVE grid cell based on the day with the largest FRE (Figures S3f and S3g in Supporting Information S1). The total fuel consumed for each FCCS pixel was estimated based on the fire danger rating of the corresponding RAVE grid cell and these were averaged to the RAVE grid (Figure S3h in Supporting Information S1). Fuel consumed associated with residual burn area (i.e., same area continuing to burn on the next day) was also included and ranged from 0% to 40% of fraction of fuel burned. These emissions estimates compare best to the Bluesky framework (Larkin et al., 2009), which also relies on the ground-based FCCS fuels data and fuel moisture (fire weather/danger).

19448007, 2026, 8, Downloaded from https://agupubs.onlinelibrary.wiley.com/doi/10.1029/2025GL120030 by Elsa M. Ordway - University Of California, Los Angeles , Wiley Online Library on [10/05/2026]. See the Terms and Conditions (https://onlinelibrary.wiley.com/terms-and-conditions) on Wiley Online Library for rules of use; OA articles are governed by the applicable Creative Commons License

10.1029/2025GL120030

19448007, 2026, 8, Downloaded from https://agupubs.onlinelibrary.wiley.com/doi/10.1029/2025GL120030 by Elsa M. Ordway - University Of California, Los Angeles , Wiley Online Library on [10/05/2026]. See the Terms and Conditions (https://onlinelibrary.wiley.com/terms-and-conditions) on Wiley Online Library for rules of use; OA articles are governed by the applicable Creative Commons License

2.5. GFED Fuel Consumed

van Wees et al. (2022) modified the GFED methodology (van der Werf et al., 2010, 2017) to generate monthly 500-m resolution global fire emissions, which we use in this work. Gridded above-ground total biomass burning carbon emissions (g C m^{-2} $month^{-1}$) are converted to fuel consumed by assuming 50% carbon content in fuel and are aggregated for the months studied (July–November 2020). Then, a similar aggregation to the RAVE grid is performed as described for FINN (Section 2.2) using GFED fuel consumed and burned area (Figure S3i in Supporting Information S1). A key difference of GFED with other methods is the use of a physically based biosphere model (the Carnegie-Ames-Stanford Approach, CASA) to quantify fuel net primary production (NPP), fuel loads, and combustion. Model inputs include satellite retrievals such as fraction of photosynthetically active radiation (fPAR), gross primary productivity (GPP), net photosynthesis (PSNnet), and tree cover. Model results are calibrated to match annual satellite based NPP, reference above- and below-ground biomass, and a database of field measurements of fuel load and consumption (van Wees et al., 2022).

3. Results and Discussion

3.1. Assessing Consistency as a Function of Burn Severity for Non-Forest Land Cover

Figure 1 shows a summary of the fuel consumed estimates for all RAVE grid cells by fuel type and average burn severity. We found large differences between burn area-based approaches for non-forested land covers. For example, mean fuel consumption between the largest and smallest estimates for low and low-moderate severity classes differ by a factor of 11–12, 12–16, and ∼10 for grassland, shrubland, and savanna, respectively. Typically, FINN fuel consumed estimates for non-forested land covers are lowest and WBSE are the highest. Tree cover in non-forests is mostly below 40% (Figure S4 in Supporting Information S1), which is below the threshold at which FINN begins to burn woody material. For these landcovers, FINN primarily burns the herbaceous vegetation with fuel loadings below 1 kg/m^2, thus explaining the low consumption estimates. In contrast, WBSE typically shows the largest fuel consumption estimates for the non-forested land covers due to multiple factors. While WBSE uses fuel loading for grasslands in the same range as those from FINN, WBSE only classifies a minor percentage of pixels as grasslands (e.g., RAVE pixels classified as grassland have, on average, less than 11% of WBSE grassland cover, see Figure S6 in Supporting Information S1), resulting in WBSE having a combination of shrubs and forest fuel with higher loadings. In addition, WBSE does not distinguish between coarse/woody and herbaceous fuels within each land cover type as do the other approaches, with the WBSE fuel loadings being closer to what is specified for coarse/woody fuels in FINN. WBSE also uses a relatively large percentage of fuel consumed (e.g., 80% for shrubs and 47%–77% for forests vs. 30% in FINN). RAVE, FCCS and GFED are typically more consistent with each other and tend to have fuel consumption values in between those from FINN and WBSE.

Based on the agreement of different methods, recommendations to some of the burn area-based approaches for the non-forest land covers can be provided. The generally low fuel consumed values from FINN compared to the other approaches are associated with two factors: (a) limiting the consumption of coarse/woody material to areas with tree cover above 40%, and (b) calculating the coarse/woody and herbaceous available fuel as the fuel loading multiplied by the fraction of the area covered by trees and non-woody vegetation, respectively. A sensitivity calculation removing both conditions (i.e., 30% of coarse/woody material is consumed regardless of tree coverage, and fuel loads for each vegetation type are assigned across the landscape) results in FINN showing comparable estimates of fuel consumed to RAVE, FCCS, and GFED for non-forest land covers (Figure S7 in Supporting Information S1). WBSE tends to show large values of fuel consumed associated to a large fraction of land cover classified as shrubland and a high fraction of fuel burned (80%) for this category. Using different underlying land cover or ecosystem classification data sets and/or modifying consumed fraction with severity could be explored to improve consistency with the other estimates.

Regardless of the differences in fuel consumed between approaches for non-forest land covers, it is notable that all of them show an increasing trend with severity as expected: The more severe the fire, the more fuel that is burned per unit area. None of the approaches include a built-in dependency of the fuel consumed with burn severity for non-forest land cover (the dependency in WBSE is only for forest), and thus this result is due to other factors. One contributor to this relationship is the robust increasing trend of % tree cover with burn severity across all land covers (Figure S4 in Supporting Information S1). While FINN has a built-in relationship with percent tree cover for the fraction of fuel consumed, a larger fraction of pixels is classified as forest on WBSE for larger % tree cover (Figure S6 in Supporting Information S1), both explaining the positive trend between fuel consumed and burn

19448007, 2026, 8, Downloaded from https://agupubs.onlinelibrary.wiley.com/doi/10.1029/2025GL120030 by Elsa M. Ordway - University Of California, Los Angeles , Wiley Online Library on [10/05/2026]. See the Terms and Conditions (https://onlinelibrary.wiley.com/terms-and-conditions) on Wiley Online Library for rules of use; OA articles are governed by the applicable Creative Commons License

severity for both estimates. While FCCS has a built-in dependency of fuel consumed with fire danger rating, we find a weak relationship between fire danger rating (SFDI) and burn severity (Figure S8 in Supporting Information S1), and thus the increasing trend of fuel consumed with burn severity for FCCS is explained for similar reasons as for WBSE. Satellite-based inputs used by GFED include tree cover and others correlated to tree cover (fPAR, GPP, and PSNnet), which also explains the relationship.

3.2. Assessing Consistency as a Function of Burn Severity for Forest Land Cover

We compare the fuel consumed across the various methods for forest land cover (Figure 1). Differences on mean fuel consumption between the largest and smallest estimates across burn severity classes are within factor of 2–3, which is lower than for non-forests but still substantial. The burn area-based approaches show increasing fuel consumed with severity, similar to the results for non-forested areas. Mean and median fuel consumed are similar for WBSE and FCCS, but FCCS has much larger variability within each burn severity class. This can be explained due to WBSE using fuel loadings for three forest categories which are based on averages of representative species (Xu et al., 2022), while FCCS uses fuel loading estimate for each of the 268 fuel beds. While FINN fuel consumption for forest areas is much larger than for non-forest due to % tree cover often being >40%, its results tend to have average fuel consumed values about a factor of 2 lower than those from WBSE and FCCS. The sensitivity calculation described in Section 3.1 also results in FINN showing comparable forest fuel consumed as WBSE and FCCS (Figure S7 in Supporting Information S1). GFED shows the largest variability within burn severity, with similar values to FINN at low severity, and similar to WBSE and FCCS at high severity.

A notable difference compared to results described in Section 3.1 is that RAVE fuel consumed for forests remains roughly constant from low to moderate-high severity and then decreases for high severity, to the point where the RAVE mean and median fall out of the inter-quartile ranges of the burn area-based approaches and thus becoming much lower than the estimates from the burn area-based approaches (Figure 1). This counterintuitive result could be associated with emissions underpredictions often found for energy-based approaches during extreme events (Byrne et al., 2024; Saide et al., 2015; van der Velde et al., 2021), which is potentially associated with sensor saturation, fire obscuration by smoke and clouds, and algorithm issues (Justice et al., 2006; Li et al., 2021a, 2022). We explore these anomalous trends more in depth in the next sections.

3.3. The Effect of Burn Duration

While cumulative FRE follows a similar trend as fuel consumed (decrease for high severity), mean FRP persistently increases with burn severity (Figure S9 in Supporting Information S1). This apparent inconsistency can be explained by a strong inverse relationship between burn duration in each RAVE grid cell and burn severity (Figure S9 in Supporting Information S1), with average burn durations of 6.6, 4.9, 3.4, and 1.6 days for “low,” “low-moderate,” “moderate-high” and “high” burn severity, respectively. In other words, high severity fires progress out of a region more quickly, while low severity fires linger for longer. While fire growth rate and burn duration are different concepts, they are likely associated, and thus these results are consistent with research showing that the fastest growing fires are also the most destructive (Balch et al., 2024). Figure 2 (left column) shows that the fuel consumed varies as a function of the burn duration for the different estimates. RAVE shows a trend of increasing fuel consumed for larger burn duration. The burn area-based estimates tend to follow this trend for “low” and “low-moderate” severity, which is associated to similar tendencies found in % tree cover for these categories (Figure S10 in Supporting Information S1) but show negative or no clear trend for more severe categories. Only FCCS shows a positive trend from <1 to 1–2 days as this is built into the calculation given the addition of residual fuel consumed after the first day. These results appear to show an increase of the fraction of fuel burned with burn duration that might not be captured by burn severity, and thus it is recommended that future work further explores these relationships to assess if burn area-based approaches need to implement it.

3.4. The Effect of Tree Cover

FRP is expected to be underpredicted for surface fires in forests due to the difficulty of sensors to penetrate the canopy and detect understory FRP (Roberts et al., 2018). We explore this effect by assessing fuel consumed as a fraction of tree cover (Figure 2, right column). The burn area-based estimates typically follow the expected trend of a continuously increasing fuel consumed with tree cover. While FINN and FCCS don't show clear trends with severity within each tree cover bin, both WBSE and GFED show the expected positive trends. While this is built into WBSE, it is notable that GFED represents this trend without using burn severity as input. Reasons of this could include the use of the CASA biosphere model for estimating fuel and consumption, but also the potential of co-correlation of the remote sensing inputs of GFED (fPAR, GPP, and PSNnet) and burn severity. On the other hand, RAVE shows different trends than the burn area-based approaches, with an increase of fuel consumed with tree cover below 40% and a sharp decrease after that. This behavior happens regardless of severity category and it's also found on other energy-based approaches (Figure S5 in Supporting Information S1). This trend is expected for low burn severity fires as they are likely occurring in the understory, for which energy-based estimates (including RAVE) do not include a correction. However, high severity fires in forested areas likely involve crown fires (USGS, 2025) making the similarly sharp decline in fuel consumed above 40% tree cover unexpected. However, this could be explained by multiple factors. First, moderate and high severity often results from scorched or brown canopy rather than from charred, black, or burned crowns (Busby et al., 2023; Meng et al., 2017). This means that in the former cases the top of the canopy did not burn and thus still contributed to FRP obstruction. Second, while satellites might be efficient at detecting the heat from flames that rise above the canopy, there will still be attenuation of the combustion happening in the understory below, and the combustion gases that absorb in the infrared (Deng et al., 2024) could additionally obstruct the signal. To our knowledge, a correction scheme that considers these effects does not exist, and thus future work is needed on this topic. When focusing on a given % tree cover bin (Figure 2, right column), fuel consumed tends to increase with severity up to "moderate-high" severity, after which there is only a slight decrease for "high" severity. Also, 71% of the "high" severity samples are in the 60%–80% tree cover range. This further emphasizes that a correction based on tree cover for moderate and high severity classes is needed.

We applied the correction developed by Roberts et al. (2018) for surface fires (bottom panel of Figure 2, see implementation details in Text S1 of Supporting Information S1) to assess the effect of this potential limitation. The correction is able to mitigate the negative trend obtained above 40% tree cover and, in some cases, reverse the decrease. Also, the correction does not affect the trends with burn duration (Figure 2, bottom-left panel). This correction is likely valid for many cases in the "low" and "low-moderate" severity categories, so it could be implemented for these cases. When implemented for fires in this study, RAVE FRE (and thus emissions) increases by a factor of 1.8 and 2.0 for "low" and "low-moderate" severity categories, respectively. We did not include corrections proposed by Roberts et al. (2018) that depend on the sensor view angle (see Text S1 in Supporting Information S1), which would only increase the estimates further and thus should be considered on future work. Considering the consistency between FCCS, WBSE, and GFAS approaches "moderate-high" and "high" severities, we could assume that these fuel consumed estimates are reasonable, which if replaced within RAVE when they are larger would result in a factor of 1.5–1.8 and 2.3–2.4 increase for "moderate-high" and "high" severities, respectively. In combination, these modifications result in a factor of 1.7–1.9 increase for RAVE emissions in forested areas. Energy-based approaches often apply scaling factors to aerosol emissions on the order of 2–4 to improve agreement with aerosol optical depth observations (Darmenov & da Silva, 2015; Kaiser et al., 2012), which could be explained partially by the findings from this work.

4. Conclusions

A key step to calculate fire emissions is to estimate the fuel consumed, which has not been thoroughly compared across approaches in the past. We compare fuel consumed from energy-based (RAVE) and burn area-based (FINN, WBSE, FCCS/Fire2Fuel, and GFED) methodologies and assess how fuel consumption changes as a function of fire and landscape characteristics. We find that all approaches show increasing fuel consumed with increased burn severity for non-forest land covers. However, their estimates can vary substantially, with differences up to factors of 10–16 in the mean between methodologies. FINN and WBSE represent extreme values for these fuel types, with RAVE, FCCS, and GFED typically falling in between. Differences between approaches are lower for forest land cover but still substantial (up to factors of 2–3 on the mean). While burn area-based approaches also show an increase in fuel consumed with burn severity for forests, the energy-based approach shows decreasing tendencies for high burn severity to a point where it mostly falls out of the range of the burn area-based approaches. Further analysis of fuel consumed from the energy-based approach shows a strong decreasing trend for tree covers above 40% for all burn severity classes. A energy-based approach driven by different satellite sensors (GFAS) shows the same trend, and thus this issue is expected to happen across energy-based approaches. This is again opposite to what is found for the burn area-based approaches. Energy-based

19448007, 2026, 8, Downloaded from https://agupubs.onlinelibrary.wiley.com/doi/10.1029/2025GL120030 by Elsa M. Ordway - University Of California, Los Angeles , Wiley Online Library on [10/05/2026]. See the Terms and Conditions (https://onlinelibrary.wiley.com/terms-and-conditions) on Wiley Online Library for rules of use; OA articles are governed by the applicable Creative Commons License

19448007, 2026, 8, Downloaded from https://agupubs.onlinelibrary.wiley.com/doi/10.1029/2025GL120030 by Elsa M. Ordway - University Of California, Los Angeles , Wiley Online Library on [10/05/2026]. See the Terms and Conditions (https://onlinelibrary.wiley.com/terms-and-conditions) on Wiley Online Library for rules of use; OA articles are governed by the applicable Creative Commons License

estimates also show an increasing fuel consumption with longer burn durations, while burn area-based estimates typically do not show this for moderate to high severity.

Recommendations to improve consistency between fuel consumption estimates vary for the evaluated model approaches. For FINN, it is recommended that available woody/coarse fuels burn even when the tree cover is less than 40%, and that fuel loads of different vegetation types (coarse/woody and herbaceous) are valid across the landscape (i.e., not scaled by the fraction of tree or herbaceous cover). These changes result in increased fuel consumed that is comparable to the energy-based approach for non-forests and to the other burn area-based approaches for forests. Use of other land cover data sets that increase the grassland land cover could help reduce fuel loads for non-forests in the WBSE estimation approach. It is also recommended that the relationship between the fraction of fuel consumed and burn duration is further explored to assess if this needs to be implemented in burn area-based approaches. In the case of the energy-based approach, a correction to account for canopy shading should be implemented for forest land covers. While these corrections exist for surface fires, parameterizations are also needed for crown fires, as our results underscore that obstruction of the signal by both the canopy and combustion gases still needs to be accounted for in these situations. We estimate that not including these corrections could result in the underprediction of FRP by almost a factor of 2, which could explain a large fraction of the scaling factor usually used by energy-based approaches to reconcile smoke concentrations. These recommendations could be implemented in energy-based approaches, but they would need to be accompanied by changes to the tuning factors currently used in each system.

A caveat of this work is that all fuel consumed used are indirect estimates. More direct estimates of fuel consumed can be obtained by using pre and post-fire LiDAR characterization (Bright et al., 2022; Hudak et al., 2020) and field surveys (Lydersen et al., 2014), which could be used in future work. The methodology described here to compare fuel consumed could also be used to evaluate and/or benchmark models coupling land surface, vegetation and fire (e.g., Ma et al., 2021), and fire-atmosphere coupled models (e.g., Turney et al., 2023) to assess their consistency with other approaches. Additionally, the recommendations provided here could be implemented in fire emissions calculations and tested within smoke modeling systems to assess potential improvements. While the domain studied is within the western and central continental U.S., it is likely that these results can be extended to other regions given the large diversity of fuels and burn severities found in the study region and the robustness of the results, which could be verified using a similar methodology in other fire-prone regions.

Conflict of Interest

The authors declare no conflicts of interest relevant to this study.

Availability Statement

RAVE (V1.0 2020) FRP and FRE data can be found in National Oceanic and Atmospheric Administration (2025). MTBS burn severity can be downloaded from MTBS (https://www.mtbs.gov/viewer/?region=all). FINNv2.5 emission files for each fire using MODIS and VIIRS were obtained from Wiedinmyer and Emmons (2022, updated irregularly). EVT and FCCS were obtained from LandFire (https://landfire.gov/data). Burning Index and Energy Release Component were obtained from Copernicus Climate Change Service Climate Data Store (2019). NLCD tree cover was available from U.S. Geological Survey (USGS) (2024). MODIS LAI, VCF and LCT are available at Myneni et al. (2021), DiMiceli et al. (2022), and Friedl and Sulla-Menashe (2022), respectively. GFAS data was retrieved from Copernicus Atmosphere Monitoring Service (2022). Data used in the analysis performed in this study can be found in Saide (2025).

Acknowledgments
This work has been supported by the following Grant NSF 2238338, NASA 80NSSC24K0300. Soja and Gargulinski were supported by NASA Grant FIRECHEM 80NSSC18K0685 and ACCDAM 80NSSC21K1456.

References

Andreae, M. O. (2019). Emission of trace gases and aerosols from biomass burning – an updated assessment. *Atmospheric Chemistry and Physics*, *19*(13), 8523–8546. https://doi.org/10.5194/acp-19-8523-2019

Balch, J. K., Iglesias, V., Mahood, A. L., Cook, M. C., Amaral, C., DeCastro, A., et al. (2024). The fastest-growing and most destructive fires in the US (2001 to 2020). *Science*, *386*(6720), 425–431. https://doi.org/10.1126/science.adk5737

Bekker, C., Salazar, M., Su, J., Garcia-Gonzales, D., Jerrett, M., Connolly, R., et al. (2025). Contribution of large wildfire events and burn severity classes to air pollution in California in 2018. *ACS ES&T Air*, *2*(7), 1148–1160. https://doi.org/10.1021/acsestair.4c00226

Bright, B. C., Hudak, A. T., McCarley, T. R., Spannuth, A., Sánchez-López, N., Ottmar, R. D., & Soja, A. J. (2022). Multitemporal LiDAR captures heterogeneity in fuel loads and consumption on the Kaibab Plateau. *Fire Ecology*, *18*(1), 18. https://doi.org/10.1186/s42408-022-00142-7

Busby, S. U., Klock, A. M., & Fried, J. S. (2023). Inventory analysis of fire effects wrought by wind-driven megafires in relation to weather and pre-fire forest structure in the western Cascades. *Fire Ecology*, *19*(1), 58. https://doi.org/10.1186/s42408-023-00219-x

Byrne, B., Liu, J., Bowman, K. W., Pascolini-Campbell, M., Chatterjee, A., Pandey, S., et al. (2024). Carbon emissions from the 2023 Canadian wildfires. *Nature*, *633*(8031), 835–839. https://doi.org/10.1038/s41586-024-07878-z

Carter, T. S., Heald, C. L., Jimenez, J. L., Campuzano-Jost, P., Kondo, Y., Moteki, N., et al. (2020). How emissions uncertainty influences the distribution and radiative impacts of smoke from fires in North America. *Atmospheric Chemistry and Physics*, *20*(4), 2073–2097. https://doi.org/10.5194/acp-20-2073-2020

Copernicus Atmosphere Monitoring Service. (2022). CAMS global biomass burning emissions based on fire radiative power (GFAS) [Dataset]. *Copernicus Atmosphere Monitoring Service (CAMS) Atmosphere Data Store*. https://doi.org/10.24381/a05253c7

Copernicus Climate Change Service Climate Data Store. (2019). Fire danger indices historical data from the copernicus emergency management service [Dataset]. *Copernicus Climate Change Service (C3S) Climate Data Store (CDS)*. https://doi.org/10.24381/cds.0e89c522

Darmenov, A., & da Silva, A. M. (2015). The quick fire emissions dataset (QFED) - Documentation of versions 2.1, 2.2 and 2.4, NASA/TM–2015–104606. Available online at https://gmao.gsfc.nasa.gov/pubs/docs/Darmenov796.pdf.*38*183

Deng, W., Zhou, M., Wang, J., Xue, Z., Lu, Z., Chen, X., et al. (2024). Advancing FRP retrieval: Bridging theory and application. *IEEE Transactions on Geoscience and Remote Sensing*, *62*, 1–16. https://doi.org/10.1109/TGRS.2024.3470538

DiMiceli, C., Sohlberg, R., & Townshend, J. (2022). MODIS/terra vegetation continuous fields yearly L3 global 250m SIN grid V061 [Dataset]. *NASA Land Processes Distributed Active Archive Center*. https://doi.org/10.5067/MODIS/MOD44B.061

Eidenshink, J., Schwind, B., Brewer, K., Zhu, Z.-L., Quayle, B., & Howard, S. (2007). A project for monitoring trends in burn severity. *Fire Ecology*, *3*(1), 3–21. https://doi.org/10.4996/fireecology.0301003

French, N. H., & Hudak, A. T. (2023). Biomass burning fuel consumption and emissions for air quality. *Landscape Fire, Smoke, and Health: Linking Biomass Burning Emissions to Human Well-Being*, *69*.

Friedl, M., & Sulla-Menashe, D. (2022). MODIS/Terra+Aqua land cover type yearly L3 global 500m SIN grid V061 [Dataset]. *NASA Land Processes Distributed Active Archive Center*. https://doi.org/10.5067/MODIS/MCD12Q1.061

Hudak, A. T., Kato, A., Bright, B. C., Loudermilk, E. L., Hawley, C., Restaino, J. C., et al. (2020). Towards spatially explicit quantification of Pre- and postfire fuels and fuel consumption from traditional and point cloud measurements. *Forest Science*, *66*(4), 428–442. https://doi.org/10.1093/forsci/fxz085

Ichoku, C., & Ellison, L. (2014). Global top-down smoke-aerosol emissions estimation using satellite fire radiative power measurements. *Atmospheric Chemistry and Physics*, *14*(13), 6643–6667. https://doi.org/10.5194/acp-14-6643-2014

Jolly, W. M., Freeborn, P. H., Page, W. G., & Butler, B. W. (2019). Severe fire danger index: A forecastable metric to inform firefighter and community wildfire risk management. *Fire*, *2*(47), 47. https://doi.org/10.3390/fire2030047

Justice, C., Giglio, L., Boschetti, L., Roy, D., Csiszar, I., Morisette, J., & Kaufman, Y. (2006). *MODIS fire products algorithm technical background document*. MODIS Science Team.

Kaiser, J. W., Heil, A., Andreae, M. O., Benedetti, A., Chubarova, N., Jones, L., et al. (2012). Biomass burning emissions estimated with a global fire assimilation system based on observed fire radiative power. *Biogeosciences*, *9*(1), 527–554. https://doi.org/10.5194/bg-9-527-2012

Larkin, N. K., O'Neill, S. M., Solomon, R., Raffuse, S., Strand, T., Sullivan, D. C., et al. (2009). The BlueSky smoke modeling framework. *International Journal of Wildland Fire*, *18*(8), 906–920. https://doi.org/10.1071/WF07086

Lee, J. M., Mirocha, J. D., Lareau, N. P., Whitney, T., To, W., Kochanski, A., & Lassman, W. (2023). Sensitivity of pyrocumulus convection to tree mortality during the 2020 creek fire in California. *Geophysical Research Letters*, *50*(16), e2023GL104193. https://doi.org/10.1029/2023GL104193

Li, F., Zhang, X., & Kondragunta, S. (2021). Highly anomalous fire emissions from the 2019–2020 Australian bushfires. *Environmental Research Communications*, *3*(10), 105005. https://doi.org/10.1088/2515-7620/ac2e6f

Li, F., Zhang, X., Kondragunta, S., Lu, X., Csiszar, I., & Schmidt, C. C. (2022). Hourly biomass burning emissions product from blended geostationary and polar-orbiting satellites for air quality forecasting applications. *Remote Sensing of Environment*, *281*, 113237. https://doi.org/10.1016/j.rse.2022.113237

Li, Y., Tong, D., Ma, S., Zhang, X., Kondragunta, S., Li, F., & Saylor, R. (2021). Dominance of wildfires impact on air quality exceedances during the 2020 record-breaking wildfire season in the United States. *Geophysical Research Letters*, *48*(21), e2021GL094908. https://doi.org/10.1029/2021GL094908

Lydersen, J. M., Collins, B. M., Ewell, C. M., Reiner, A. L., Fites, J. A., Dow, C. B., et al. (2014). Using field data to assess model predictions of surface and ground fuel consumption by wildfire in coniferous forests of California. *Journal of Geophysical Research: Biogeosciences*, *119*(3), 223–235. https://doi.org/10.1002/2013JG002475

Ma, W., Zhai, L., Pivovaroff, A., Shuman, J., Buotte, P., Ding, J. Y., et al. (2021). Assessing climate change impacts on live fuel moisture and wildfire risk using a hydrodynamic vegetation model. *Biogeosciences*, *18*(13), 4005–4020. https://doi.org/10.5194/bg-18-4005-2021

Mattarochia, K. A. (2022). Interactive decision support services and case review of the creek fire during COVID-19. In *American meteorological society meeting abstracts, 2022, 3.5*.

Meng, R., Wu, J., Schwager, K. L., Zhao, F., Dennison, P. E., Cook, B. D., et al. (2017). Using high spatial resolution satellite imagery to map forest burn severity across spatial scales in a pine barrens ecosystem. *Remote Sensing of Environment*, *191*, 95–109. https://doi.org/10.1016/j.rse.2017.01.016

Myneni, R., Knyazikhin, Y., & Park, T. (2021). MODIS/terra+Aqua leaf area Index/FPAR 4-Day L4 global 500m SIN grid V061 [Dataset]. *NASA Land Processes Distributed Active Archive Center*. https://doi.org/10.5067/MODIS/MCD15A3H.061

National Oceanic and Atmospheric Administration. (2025). Hourly regional ABI and VIIRS fire emissions (RAVE) across North America (V1.0 2020) [Dataset]. *Zenodo*. https://doi.org/10.5281/zenodo.17364332

Ottmar, R. D., Sandberg, D. V., Riccardi, C. L., & Prichard, S. J. (2007). An overview of the fuel characteristic classification system — Quantifying, classifying, and creating fuelbeds for resource planningThis article is one of a selection of papers published in the special forum on the fuel characteristic classification system. *Canadian Journal of Forest Research*, *37*(12), 2383–2393. https://doi.org/10.1139/x07-077

Pan, X., Ichoku, C., Chin, M., Bian, H., Darmenov, A., Colarco, P., et al. (2020). Six global biomass burning emission datasets: Intercomparison and application in one global aerosol model. *Atmospheric Chemistry and Physics*, *20*(2), 969–994. https://doi.org/10.5194/acp-20-969-2020

Parrington, M., Whaley, C. H., French, N. H. F., Buchholz, R. R., Pan, X., Wiedinmyer, C., et al. (2025). Biomass burning emission estimation in the MODIS era: State-of-the-art and future directions. *Elementa: Science of the Anthropocene*, *13*(1), 00089. https://doi.org/10.1525/elementa.2024.00089

Petrenko, M., Kahn, R., Chin, M., Soja, A., & Kucsera, T. (2012). Harshvardhan: The use of satellite-measured aerosol optical depth to constrain biomass burning emissions source strength in the global model GOCART. *Journal of Geophysical Research*, *117*, D18212. https://doi.org/10.1029/2012jd017870

19448007, 2026, 8, Downloaded from https://agupubs.onlinelibrary.wiley.com/doi/10.1029/2025GL120030 by Elsa M. Ordway - University Of California, Los Angeles , Wiley Online Library on [10/05/2026]. See the Terms and Conditions (https://onlinelibrary.wiley.com/terms-and-conditions) on Wiley Online Library for rules of use; OA articles are governed by the applicable Creative Commons License

Pierce, R. B., Schaack, T., Al-Saadi, J. A., Fairlie, T. D., Kittaka, C., Lingenfelser, G., et al. (2007). Chemical data assimilation estimates of continental U.S. ozone and nitrogen budgets during the intercontinental chemical transport experiment–north America. *Journal of Geophysical Research*, *112*(D12), D12S21. https://doi.org/10.1029/2006jd007722

Riccardi, C. L., Ottmar, R. D., Sandberg, D. V., Andreu, A., Elman, E., Kopper, K., & Long, J. (2007). The fuelbed: A key element of the fuel characteristic classification SystemThis article is one of a selection of papers published in the special forum on the fuel characteristic classification system. *Canadian Journal of Forest Research*, *37*(12), 2394–2412. https://doi.org/10.1139/x07-143

Roberts, G., Wooster, M. J., Lauret, N., Gastellu-Etchegorry, J. P., Lynham, T., & McRae, D. (2018). Investigating the impact of overlying vegetation canopy structures on fire radiative power (FRP) retrieval through simulation and measurement. *Remote Sensing of Environment*, *217*, 158–171. https://doi.org/10.1016/j.rse.2018.08.015

Safford, H. D., Paulson, A. K., Steel, Z. L., Young, D. J. N., & Wayman, R. B. (2022). The 2020 California fire season: A year like no other, a return to the past or a harbinger of the future? *Global Ecology and Biogeography*, *31*(10), 2005–2025. https://doi.org/10.1111/geb.13498

Saide, P. E. (2025). Assessing consistency in fuel consumed between activity-based wildfire emission estimates [Dataset]. *Zenodo*. https://doi.org/10.5281/zenodo.17342810

Saide, P. E., Peterson, D., da Silva, A., Anderson, B., Ziemba, L. D., Diskin, G., et al. (2015). Revealing important nocturnal and day-to-day variations in fire smoke emissions through a multiplatform inversion. *Geophysical Research Letters*, *42*(9), 3609–3618. https://doi.org/10.1002/2015gl063737

Seiler, W., & Crutzen, P. J. (1980). Estimates of gross and net fluxes of carbon between the biosphere and the atmosphere from biomass burning. *Climatic Change*, *2*(3), 207–247. https://doi.org/10.1007/BF00137988

Shi, Y., Matsunaga, T., Saito, M., Yamaguchi, Y., & Chen, X. (2015). Comparison of global inventories of CO2 emissions from biomass burning during 2002–2011 derived from multiple satellite products. *Environmental Pollution*, *206*, 479–487. https://doi.org/10.1016/j.envpol.2015.08.009

Soja, A. J., Cofer, W. R., Shugart, H. H., Sukhinin, A. I., Stackhouse, P. W., Jr., McRae, D. J., & Conard, S. G. (2004). Estimating fire emissions and disparities in boreal siberia (1998–2002). *Journal of Geophysical Research*, *109*(D14). https://doi.org/10.1029/2004JD004570

Stockwell, C. E., Bela, M. M., Coggon, M. M., Gkatzelis, G. I., Wiggins, E., Gargulinski, E. M., et al. (2022). Airborne emission rate measurements validate remote sensing observations and emission inventories of Western U.S. wildfires. *Environmental Science & Technology*, *56*(12), 7564–7577. https://doi.org/10.1021/acs.est.1c07121

Turney, F. A., Saide, P. E., Jimenez Munoz, P. A., Muñoz-Esparza, D., Hyer, E. J., Peterson, D. A., et al. (2023). Sensitivity of burned area and fire radiative power predictions to containment efforts, fuel density, and fuel moisture using WRF-fire. *Journal of Geophysical Research: Atmospheres*, *128*(18), e2023JD038873. https://doi.org/10.1029/2023JD038873

U.S. Geological Survey (USGS). (2024). Annual NLCD Collection 1 science products [Dataset]. *U.S. Geological Survey data release*. https://doi.org/10.5066/P94UXNTS

USGS. (2025). Post-fire mapping glossary. Retrieved from https://burnseverity.cr.usgs.gov/glossary

van der Velde, I. R., van der Werf, G. R., Houweling, S., Maasakkers, J. D., Borsdorff, T., Landgraf, J., et al. (2021). Vast CO2 release from Australian fires in 2019–2020 constrained by satellite. *Nature*, *597*(7876), 366–369. https://doi.org/10.1038/s41586-021-03712-y

van der Werf, G. R., Randerson, J. T., Giglio, L., Collatz, G. J., Mu, M., Kasibhatla, P. S., et al. (2010). Global fire emissions and the contribution of deforestation, savanna, forest, agricultural, and peat fires (1997–2009). *Atmospheric Chemistry and Physics*, *10*(23), 11707–11735. https://doi.org/10.5194/acp-10-11707-2010

van der Werf, G. R., Randerson, J. T., Giglio, L., van Leeuwen, T. T., Chen, Y., Rogers, B. M., et al. (2017). Global fire emissions estimates during 1997–2016. *Earth System Science Data*, *9*(2), 697–720. https://doi.org/10.5194/essd-9-697-2017

van Wees, D., van der Werf, G. R., Randerson, J. T., Rogers, B. M., Chen, Y., Veraverbeke, S., et al. (2022). Global biomass burning fuel consumption and emissions at 500 m spatial resolution based on the global fire emissions database (GFED). *Geoscientific Model Development*, *15*(22), 8411–8437. https://doi.org/10.5194/gmd-15-8411-2022

Warneke, C., Schwarz, J. P., Dibb, J., Kalashnikova, O., Frost, G., Al-Saad, J., et al. (2023). Fire influence on regional to global environments and air quality (FIREX-AQ). *Journal of Geophysical Research: Atmospheres*, *128*(2), e2022JD037758. https://doi.org/10.1029/2022JD037758

Wiedinmyer, C., Akagi, S. K., Yokelson, R. J., Emmons, L. K., Al-Saadi, J. A., Orlando, J. J., & Soja, A. J. (2011). The fire INventory from NCAR (FINN): A high resolution global model to estimate the emissions from open burning. *Geoscientific Model Development*, *4*(3), 625–641. https://doi.org/10.5194/gmd-4-625-2011

Wiedinmyer, C., & Emmons, L. (2022). Fire inventory from NCAR version 2 fire emission [Dataset]. *NSF National Center for Atmospheric Research*. https://doi.org/10.5065/XNPA-AF09

Wiedinmyer, C., Kimura, Y., McDonald-Buller, E. C., Emmons, L. K., Buchholz, R. R., Tang, W., et al. (2023). The fire inventory from NCAR version 2.5: An updated global fire emissions model for climate and chemistry applications. *Geoscientific Model Development*, *16*(13), 3873–3891. https://doi.org/10.5194/gmd-16-3873-2023

Wiggins, E. B., Anderson, B. E., Brown, M. D., Campuzano-Jost, P., Chen, G., Crawford, J., et al. (2021). Reconciling assumptions in Bottom-Up and top-down approaches for estimating aerosol emission rates from wildland fires using observations from FIREX-AQ. *Journal of Geophysical Research: Atmospheres*, *126*(24), e2021JD035692. https://doi.org/10.1029/2021JD035692

Williams, A. P., Juang, C. S., & Short, K. C. (2025). The Western United States MTBS-interagency database of large wildfires, 1984–2024 (WUMI2024a). *Earth System Science Data Discussions*, 1–21. https://doi.org/10.5194/essd-2025-366

Wooster, M. J., Roberts, G., Perry, G. L. W., & Kaufman, Y. J. (2005). Retrieval of biomass combustion rates and totals from fire radiative power observations: FRP derivation and calibration relationships between biomass consumption and fire radiative energy release. *Journal of Geophysical Research*, *110*(D24), D24311. https://doi.org/10.1029/2005jd006318

Xu, Q., Westerling, A. L., Notohamiprodjo, A., Wiedinmyer, C., Picotte, J. J., Parks, S. A., et al. (2022). Wildfire burn severity and emissions inventory: An example implementation over California. *Environmental Research Letters*, *17*(8), 085008. https://doi.org/10.1088/1748-9326/ac80d0

Ye, X., Arab, P., Ahmadov, R., James, E., Grell, G. A., Pierce, B., et al. (2021). Evaluation and intercomparison of wildfire smoke forecasts from multiple modeling systems for the 2019 Williams flats fire. *Atmospheric Chemistry and Physics*, *21*(18), 14427–14469. https://doi.org/10.5194/acp-21-14427-2021

Zhang, F., Wang, J., Ichoku, C., Hyer, E. J., Yang, Z., Ge, C., et al. (2014). Sensitivity of mesoscale modeling of smoke direct radiative effect to the emission inventory: A case study in northern sub-saharan African region. *Environmental Research Letters*, *9*(7), 075002. https://doi.org/10.1088/1748-9326/9/7/075002

19448007, 2026, 8, Downloaded from https://agupubs.onlinelibrary.wiley.com/doi/10.1029/2025GL120030 by Elsa M. Ordway - University Of California, Los Angeles , Wiley Online Library on [10/05/2026]. See the Terms and Conditions (https://onlinelibrary.wiley.com/terms-and-conditions) on Wiley Online Library for rules of use; OA articles are governed by the applicable Creative Commons License

References From the Supporting Information

Asner, G. P., Scurlock, J. M. O., & Hicke, J. A. (2003). Global synthesis of leaf area index observations: Implications for ecological and remote sensing studies. *Global Ecology and Biogeography*, *12*(3), 191–205. https://doi.org/10.1046/j.1466-822X.2003.00026.x

Carroll, M., Townshend, J., Hansen, M., DiMiceli, C., Sohlberg, R., & Wurster, K. (2011). MODIS vegetative cover conversion and vegetation continuous fields. In B. Ramachandran, C. O. Justice, & M. J. Abrams (Eds.), *Land remote sensing and global environmental change: NASA's Earth observing system and the science of ASTER and MODIS* (pp. 725–745). Springer New York.

Di Giuseppe, F., Pappenberger, F., Wetterhall, F., Krzeminski, B., Camia, A., Libertá, G., & San Miguel, J. (2016). The potential predictability of fire danger provided by numerical weather prediction. *Journal of Applied Meteorology and Climatology*, *55*(11), 2469–2491. https://doi.org/10.1175/JAMC-D-15-0297.1

Friedl, M. A., Sulla-Menashe, D., Tan, B., Schneider, A., Ramankutty, N., Sibley, A., & Huang, X. (2010). MODIS Collection 5 global land cover: Algorithm refinements and characterization of new datasets. *Remote Sensing of Environment*, *114*(1), 168–182. https://doi.org/10.1016/j.rse.2009.08.016

Houseman, I., Schleeweis, K., Heyer, J., Ruefenacht, B., Bender, S., Megown, K., et al. (2023). *National land cover database tree canopy cover methods*. US Department of Agriculture, Forest Service, Geospatial Technology and Applications Center.

Kahiu, M. N., & Hanan, N. P. (2018). Estimation of woody and herbaceous leaf area index in Sub-Saharan Africa using MODIS data. *Journal of Geophysical Research: Biogeosciences*, *123*(1), 3–17. https://doi.org/10.1002/2017JG004105

Knyazikhin, Y., Martonchik, J. V., Myneni, R. B., Diner, D. J., & Running, S. W. (1998). Synergistic algorithm for estimating vegetation canopy leaf area index and fraction of absorbed photosynthetically active radiation from MODIS and MISR data. *Journal of Geophysical Research*, *103*(D24), 32257–32275. https://doi.org/10.1029/98JD02462

Rollins, M. G. (2009). LANDFIRE: A nationally consistent vegetation, wildland fire, and fuel assessment. *International Journal of Wildland Fire*, *18*(3), 235–249. https://doi.org/10.1071/WF08088

19448007, 2026, 8, Downloaded from https://agupubs.onlinelibrary.wiley.com/doi/10.1029/2025GL120030 by Elsa M. Ordway - University Of California, Los Angeles , Wiley Online Library on [10/05/2026]. See the Terms and Conditions (https://onlinelibrary.wiley.com/terms-and-conditions) on Wiley Online Library for rules of use; OA articles are governed by the applicable Creative Commons License